



ELSEVIER

Journal of Materials Processing Technology 95 (1999) 238–245

Journal of
**Materials
Processing
Technology**

www.elsevier.com/locate/jmatprotec

Residual stresses in ground components caused by coupled thermal and mechanical plastic deformation

M. Mahdi, L.C. Zhang*

Department of Mechanical and Mechatronic Engineering, The University of Sydney, Sydney, NSW 2006, Australia

Received 15 May 1998

Abstract

The purpose of this paper is to understand the combined effect of thermal and mechanical plastic deformation on residual stresses in ground components. The interactions between a grinding wheel and a workpiece, including both thermal and mechanical interaction, are simulated by triangular surface loads moving with the table speed of grinding. Cooling is modelled by a uniform convection over the grinding surface. It was found that the residual stress distribution is sensitive to some combination of grinding conditions. As the surface residual stresses are concerned, a down-grinding is of advantage when the ratio of horizontal to vertical forces is low, the input heat flux is intermediate and the vertical mechanical traction is high. Under a high heat flux input, a compressive residual stress distribution can be achieved if either the table speed or convection heat transfer coefficient is high. © 1999 Elsevier Science S.A. All rights reserved.

Keywords: Residual stresses; Grinding; Coupling effect; Mechanical loading; Thermal loading; Plastic deformation

1. Introduction

Mechanical-plastic deformation and thermal-plastic deformation are two major factors in the formation of residual stresses in a ground component [1]. In the previous parts of their series studies, the authors have developed an adaptive numerical approach to analyse grinding-induced temperature field [2] and have investigated the residual stresses caused by surface mechanical loading [3] and thermal-plastic deformation [4] individually. They showed that when thermal-plastic deformation was the only source of residual stresses the hypothesis of temperature-independent properties would underestimate thermal-plastic deformation and that the Peclet number had a significant effect on the selection of critical grinding conditions. However, when the mechanical-plastic deformation was the only factor involved, the grinding-induced residual stresses were sensitive to the profile of surface traction. To generate compressive surface residual stresses, in this case, they recommended using down-grinding operations with sufficiently large ratio of horizontal to vertical forces and smaller depth of cut.

Under a wide range of grinding conditions, however, mechanical-plastic deformation and thermal-plastic deformation

can occur simultaneously. The coupling of the two types of permanent deformation may change the nature of residual stresses. Thus from a practical point of view, it is necessary to examine the mechanism of residual stress formation in a workpiece when the coupling of thermal-mechanical deformation happens. This paper aims to understand the effect of these two types of deformation in grinding on the variation of residual stresses.

2. The finite element modelling

2.1. Problem description

As discussed in previous studies [2–4], the deformation of a workpiece subjected to a surface grinding operation can be considered as a plane-strain problem, as shown in Fig. 1. Both theoretical and experimental studies [5] have shown that the heat generated in grinding can be approximated reasonably by a triangular heat flux, q , moving along the positive direction of x -axis on the workpiece surface [2–5]. Similarly, the interaction stresses between the grinding wheel and workpiece can also be simulated by surface traction stresses with triangular profiles [6]. The peaks of surface traction and heat flux have the same local coordinate, ξ_a , which represents the mechanics of deformation. The horizontal grinding traction can be assumed to be propor-

*Corresponding author. Tel.: +61-2-9351-2835; fax: +61-2-9351-3760
E-mail address: zhang@mech.eng.usyd.edu.au (L.C. Zhang)

Table 1
Composition and properties of EN23 steel

Composition (wt%)						Yield stress (MPa)	Young's modulus (GPa)	Thermal coefficient of expansion (C^{-1})	Poisson's ratio
C	Si	Mn	Cr	Mo	Ni				
0.3	0.25	0.55	0.71	0.06	3.41	796	214	1.45×10^{-5}	0.27

tional to the vertical throughout the grinding zone. Thus in this study the ratio of the horizontal traction to the vertical, μ , is introduced to facilitate the finite element analysis using consistent nodal forces.

With the modelling technique described above, up- and down-grinding processes can be distinguished easily in the mechanics analysis using the finite element method. For an up-grinding operation, the direction of the horizontal nodal forces is positive but for a down-grinding it becomes negative. In addition, the peak locations of surface traction and heat flux vary with types of grinding processes. The relative peak location l_a , which is defined as $2\zeta_a/L_c$ where L_c is the grinding zone length, is in the interval (0,0.5) for an up-grinding and (0.5,1.0) for a down-grinding. Thus in the present study, $l_a = 0.25$ and 0.75 are used to count for the difference of the two grinding processes.

The influence of cooling fluid is reflected by a uniform heat convection over the whole grinding surface, as shown in Fig. 1. To compare the coupling effect on residual stresses with those caused by individual mechanical or thermal deformation, EN23 steel [7], which has been used in the previous studies of the authors [2–4], is still used in the present paper as the workmaterial. Its properties and compositions are listed in Table 1.

2.2. Control volume and error analysis

One must use a large control volume to eliminate the boundary effect due to mechanical and thermal loadings. In this study, a control volume with dimensions of $24L_c \times 24L_c$ is applied with the first layer of $0.5L_c$ in depth being divided into eight sub-layers to smoothly model the residual stresses

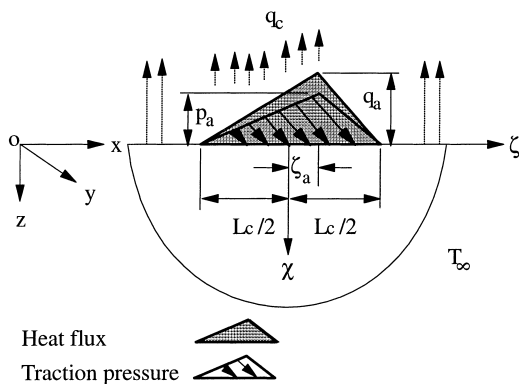


Fig. 1. A theoretical model of surface grinding with convection.

distribution. The control volume is discretized by 1248 nine node-quadratic elements and 5211 nodes. Fig. 2 (a) and (b) show that a finer mesh produces a smoother residual stress distribution. Fig. 2 (c) demonstrates that the resultant horizontal force arising from the longitudinal residual stress σ_{xx} is nearly zero and therefore depth of the control volume used is adequate.

Reliable residual stresses can only be obtained when both the mechanical and thermal loads have moved away for a long period of time, ie., when a state free from external loading in the workpiece has been achieved. To facilitate numerical simulation using the finite element method, a total of 132 solution steps are used in the present study to approximate the complete cooling and unloading conditions. The temperature rise of grinding and the surface traction are drawn back to zero linearly in the last 20 solution steps. Fig. 3 confirms that the above solution steps are sufficient as both the temperature rise of grinding and stress components approach their steady states quickly. The nearly flat surface residual stress distribution in Fig. 3 (c) indicates that good approximation of residual stresses can be obtained.

3. Results and discussion

3.1. Onset of plastic deformation

Residual stresses appear when any irreversible deformation, which is the plastic deformation in the present study, takes place. If the onset of plastic deformation is predicted by the the maximum effective stress according to the von Mises yield criteria, it found that the onset of plastic deformation in grinding is mainly a function of the intensity of heat source if the mechanical surface traction is low, say below $0.5Y$ (see Fig. 4). At a relatively high surface traction, however, the effect of heat source intensity becomes less dominant, particularly when the ratio of horizontal to normal mechanical traction is high, eg, $|\mu| = 0.3$. Moreover, the type of grinding operations, ie., up- or down-grinding, has little influence on the onset of plastic deformation.

3.2. Residual stresses

There are two major surface residual stresses, σ_{xx} and σ_{yy} ¹, and the magnitudes of which are directly related to the

¹The shearing stress σ_{xy} is very small compared with σ_{xx} and σ_{yy} and thus will not be discussed.

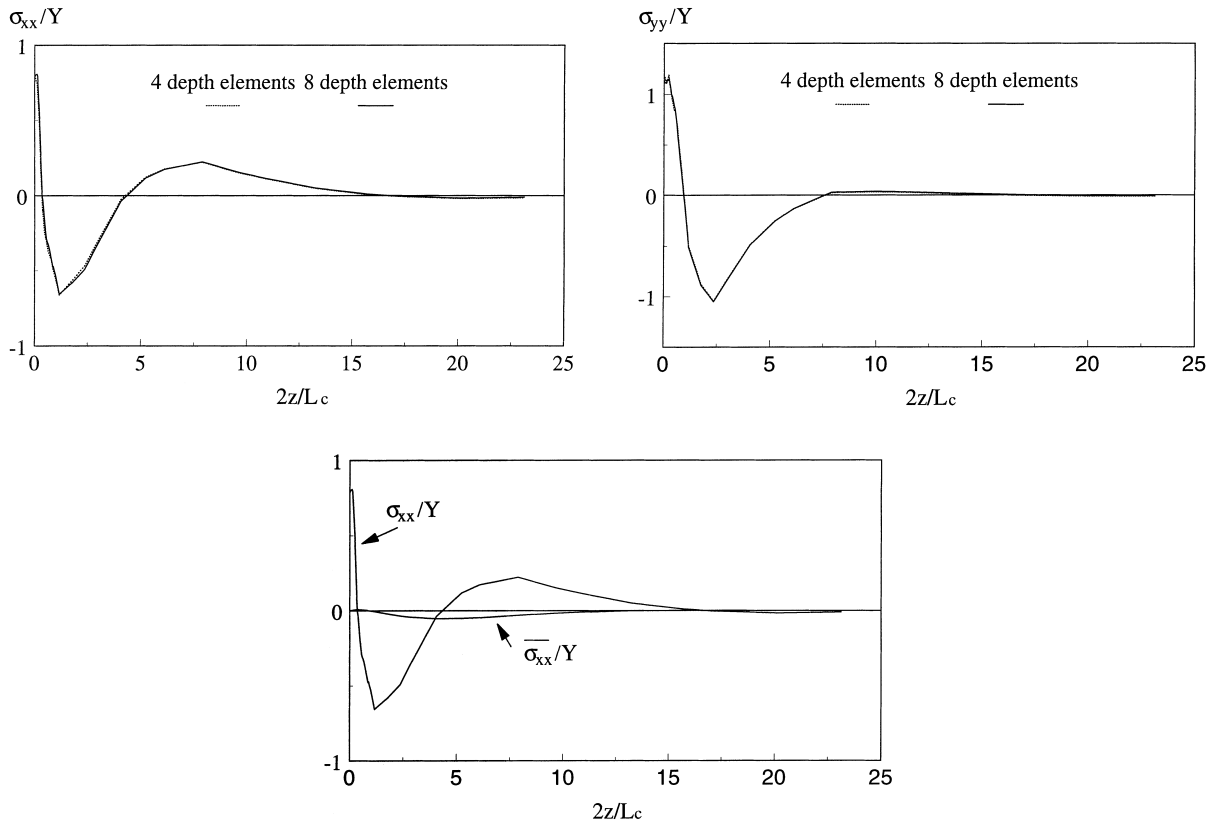


Fig. 2. FEA mesh refining and control volume accuracy ($H_\infty = 0$, $l_a = 0.25$, $Pe_\infty = 1$ and $q_a = 80 \text{ MW/m}^2$, $p_a = 2Y$): (a) relative error in longitudinal stress, σ_{xx} ; (b) relative error in plane stress, σ_{yy} ; (c) balance of the longitudinal stress, σ_{xx} .

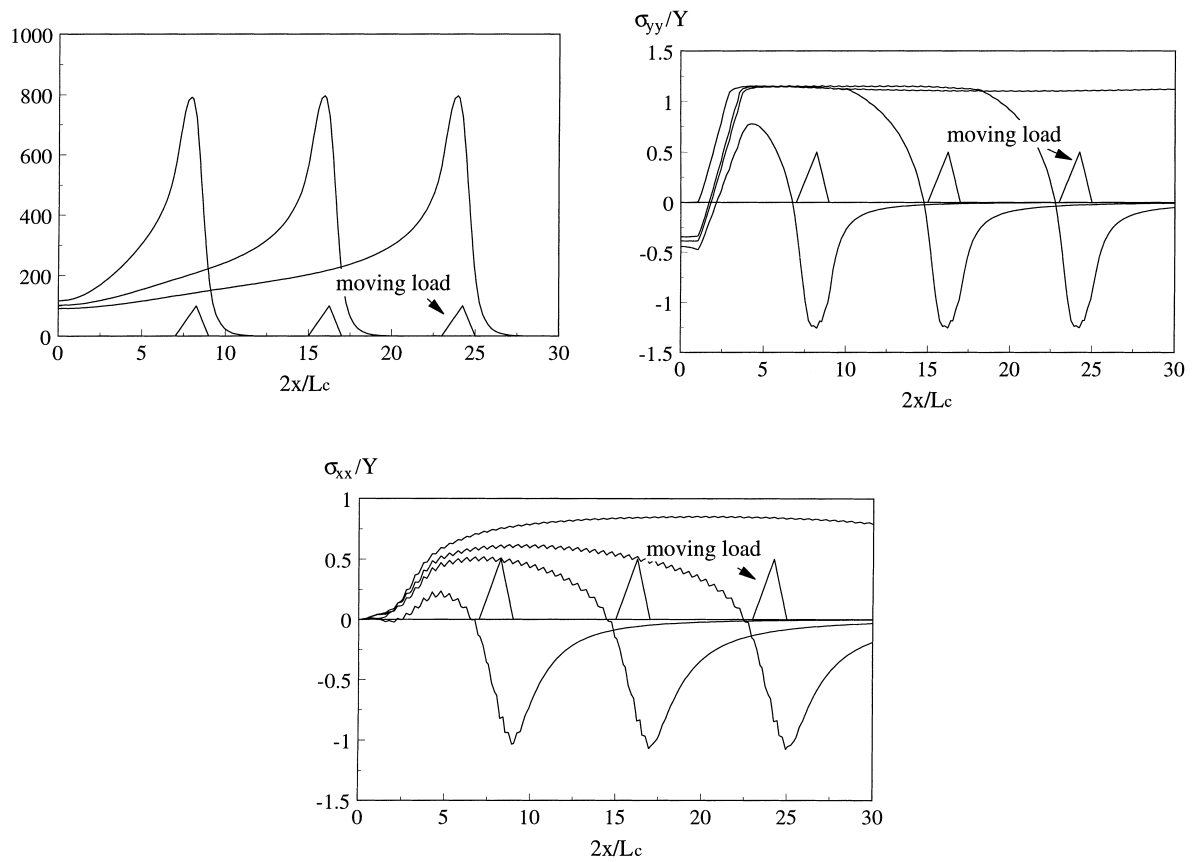


Fig. 3. A typical history of grinding surface temperature and stresses ($H = 0.0$, $l_a = 0.25$, $Pe = 1$, $q_a = 50 \text{ MW/m}^2$, $p_a = 0.125Y$, $\mu = 0.1$): (a) surface temperature; (b) σ_{xx} ; (c) σ_{yy} .

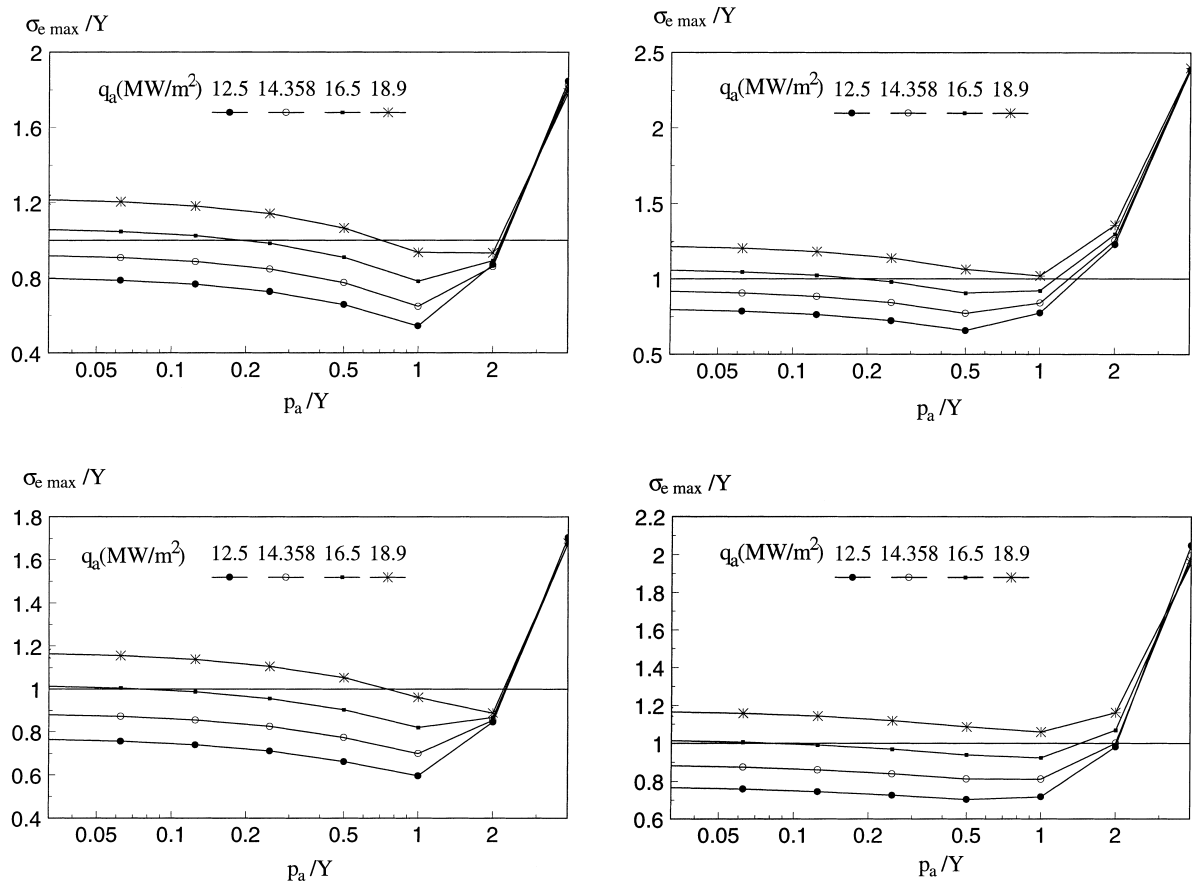


Fig. 4. Thermo-mechanical grinding conditions and maximum effective stress ($Pe = 1, H = 0$): (a) $\sigma_{e \max}$, ($l_a = 0.25, \mu = 0.1$); (b) $\sigma_{e \max}$, ($l_a = 0.25, \mu = 0.3$); (c) $\sigma_{e \max}$, ($l_a = 0.75, \mu = 0.1$); (d) $\sigma_{e \max}$, ($l_a = 0.75, \mu = 0.3$).

grinding conditions. As shown in Fig. 5, greater traction may decrease the magnitudes of both the residual stresses if the ratio of the horizontal to vertical traction is low (eg, $|\mu| = 0.1$). This is attributed to the relaxation of the initial surface compressive stresses generated by heating in the grinding zone, which in turn reduces the total longitudinal strain and surface stresses. For a high μ (eg, $= 0.3$), a greater surface traction would lead to an undesirable residual stress distribution (see Fig. 5(e) and (f)). This is because the surface workmaterial in the grinding zone experienced a greater initial surface stretching and thus a larger tensile stress, σ_{xx} , during grinding. In this sense, therefore, an up-grinding operation is advantageous in terms of residual stresses if a lower heat flux input and a smaller μ can be maintained.

Fig. 6 indicates that a down-grinding mechanism introduces smaller surface residual stresses if the peak of the vertical surface traction is below the yield stress of the workmaterial, ie., if $p_a/Y < 1$. It is understandable as the thermal residual stresses must become dominant when $p_a/Y < 1$ and grinding temperature associated with a down-grinding process is less than that with an up-grinding. If p_a is high (but $p_a/Y \leq 2$), however, an up-grinding results in less residual stresses and therefore is more favourable.

The increase of the heat flux intensity elevates the grinding temperature and in turn enlarges the thermal strains. It is apparent according to Fig. 6(c) and (d) that the coupling of mechanical traction with a high input of heat flux has a similar effect to that of pure thermal loading conditions, because greater surface residual stresses are generated. It should be noted that the grinding temperature in down-grinding is lower so that a down-grinding produces less residual stresses. This is similar to the results with smaller $p_a/Y < 1$, as shown in Fig. 6(a) and (b). In addition, the increase of mechanical traction increases the longitudinal residual stress, σ_{xx} , but has little effect on the plane residual stress, σ_{yy} .

Cooling due to grinding fluid has a remarkable effect on residual stresses. Fig. 7 shows the results of an up-grinding process when the convection heat transfer coefficient, H , increases and when the maximum grinding temperature remains the same as in the case studies discussed above.² The results indicate that a higher traction can decrease the residual stresses and even a state of no residual stresses can be achieved when $p_a/Y = 2$. The mechanism of such an

²To achieve such a condition, a high input heat flux with $q_a = 43.25 \text{ MW/m}^2$ is applied.

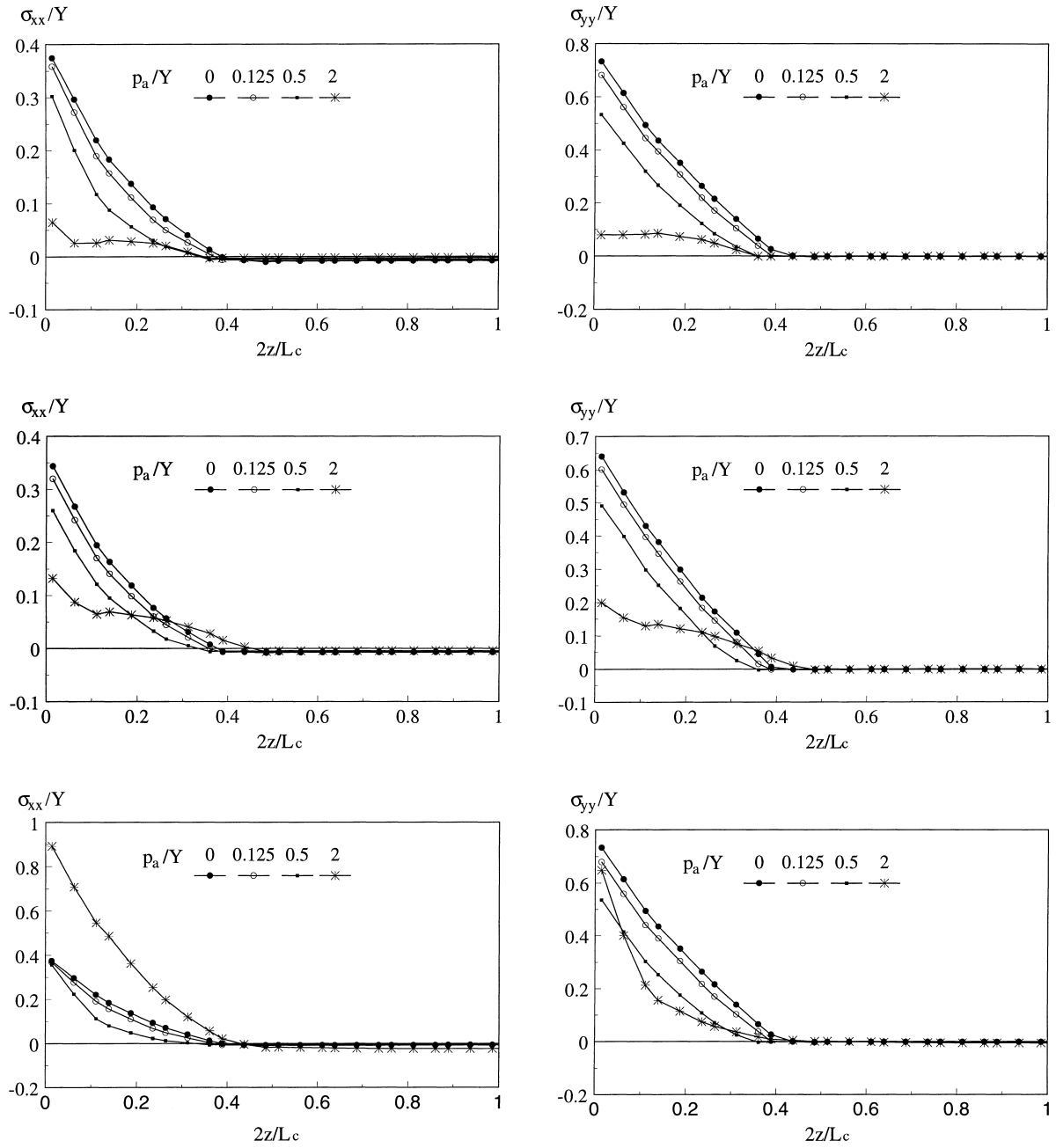


Fig. 5. Typical thermo-mechanical residual stress distributions ($H = 0.0$, $l_a = 0.25$, $Pe = 1$, $q_a = 25 \text{ MW/m}^2$): (a) σ_{xx} , ($l_a = 0.25$, $\mu = 0.1$); (b) σ_{yy} , ($l_a = 0.25$, $\mu = 0.1$); (c) σ_{xx} , ($l_a = 0.75$, $\mu = 0.1$); (d) σ_{yy} , ($l_a = 0.75$, $\mu = 0.1$); (e) σ_{xx} , ($l_a = 0.75$, $\mu = 0.3$); (f) σ_{yy} , ($l_a = 0.75$, $\mu = 0.3$).

interesting phenomenon can be elucidated when the stress variation with the motion of surface traction is monitored. As shown in Fig. 8(a), in the early stages of the traction motion, eg, at $2x_c/L_c = 8$ where x_c is the coordinate of the traction centre, the longitudinal stress is slightly tensile. With further movement of the traction the stress becomes compressive. The reason behind is related to the role of thermal and mechanical strains. At an early stage (Case 1 of Fig. 8(a)), the ground surface is subjected to mechanical stretching strains higher than those of thermal origin together with constrains from deep layers. Therefore a

tensile stress is developed. In later stages (Case 2 and Case 3 in Fig. 8(a)), the mechanical strains become much less than the thermal strains, which in turn forces the ground surface to expand and thus a compressive surface stress develops. The plane stress σ_{yy} remains tensile due to the dominant effect of mechanical shear strains caused the horizontal grinding force (see Fig. 8(b)). It is clear that both the stress components vanish as the traction moves away. For a deeper understanding of the above mechanism, the residual stresses induced by sole sources, ie., by only mechanical or thermal deformation, are analysed and compared with those due to

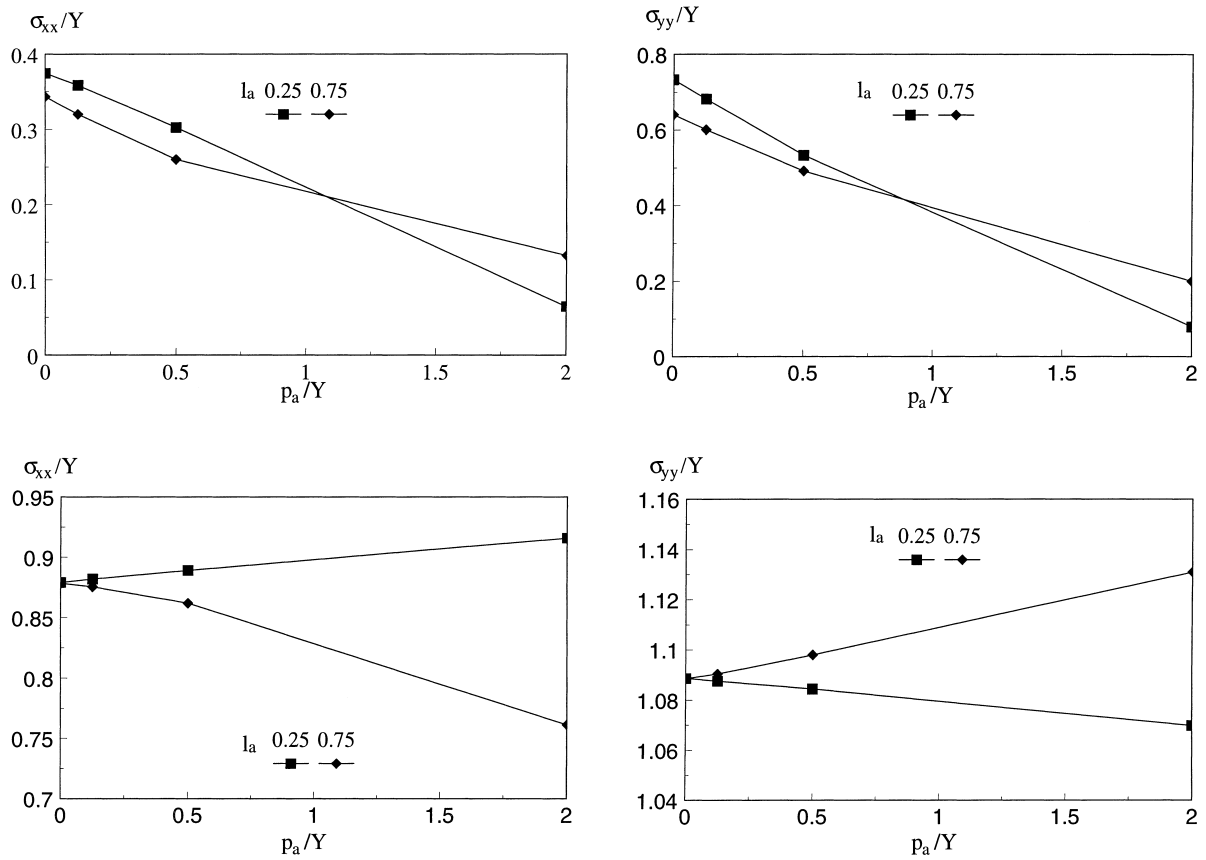


Fig. 6. Surface thermo-mechanical residual stresses and type of grinding ($H = 0.0$, $Pe = 1$, $\mu = 0.1$): (a) σ_{xx} , ($q_a = 25 \text{ MW/m}^2$); (b) σ_{yy} , ($q_a = 25 \text{ MW/m}^2$); (c) σ_{xx} , ($q_a = 50 \text{ MW/m}^2$); (d) σ_{yy} , ($q_a = 50 \text{ MW/m}^2$).

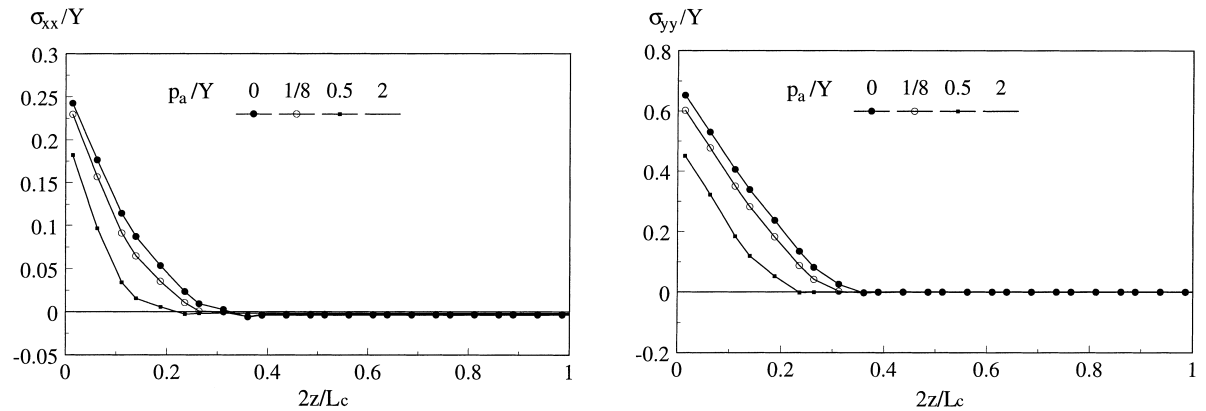


Fig. 7. Cooling effect on residual stress distributions ($H = 1.0$, $l_a = 0.25$, $Pe = 1$, $q_a = 43.25 \text{ MW/m}^2$, $\mu = 0.1$): (a) σ_{xx} ; (b) σ_{yy} .

the coupled effect, as illustrated in Fig. 9. The thermal residual stresses are tensile. But the sole mechanical residual stresses are negligible compared with the thermal. However, the coupling of mechanical deformation with thermal deformation results in a residual stress free state. This clearly indicates that the coupling is very non-linear.

The increase of table speed results in a higher material removal and consequently generates a higher heat input.

When table speed is sufficiently large, more heat is diffused in the direction of grinding which in turn results in a more localised temperature rise in the vicinity of the workpiece surface but reduces the maximum grinding temperature. Fig. 10 shows that the effect of increasing the table speed and convection heat transfer coefficient has similar influence on the residual stresses with coupled thermal-mechanical properties.

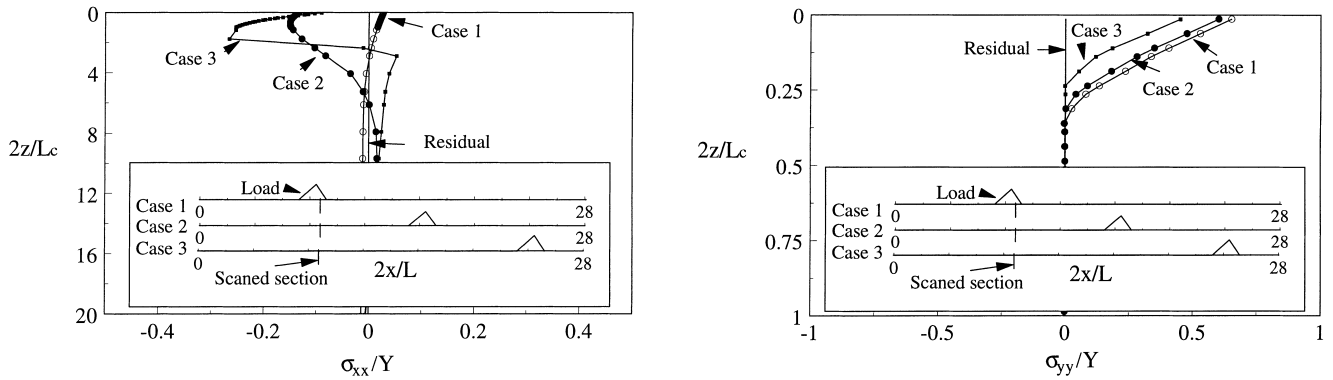


Fig. 8. Thermo-mechanical stress history ($H = 1.0$, $l_a = 0.25$, $Pe = 1$, $q_a = 43.25 \text{ MW/m}^2$, $\mu = 0.1$, $p_a = 2Y$): (a) σ_{xx} ; (b) σ_{yy} .

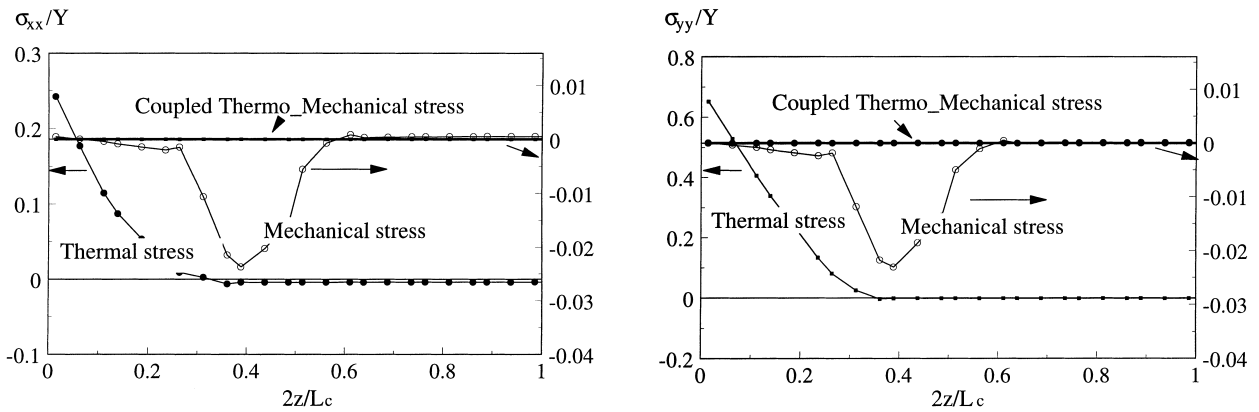


Fig. 9. Coupling mechanism ($H = 1.0$, $l_a = 0.25$, $Pe = 1$, $q_a = 43.25 \text{ MW/m}^2$, $\mu = 0.1$, $p_a = 2Y$): (a) σ_{xx} ; (b) σ_{yy} .

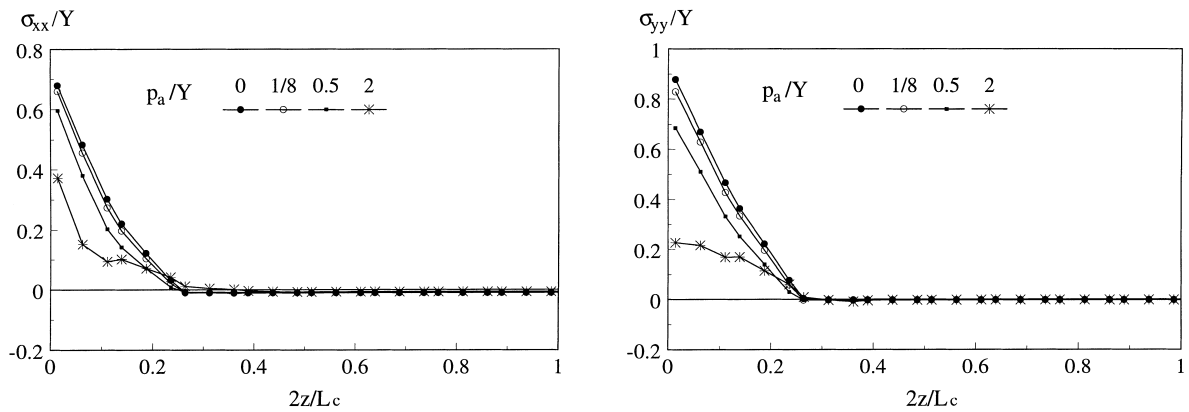


Fig. 10. The table speed effect ($H = 1.0$, $l_a = 0.25$, $Pe = 1$, $q_a = 43.25 \text{ MW/m}^2$, $\mu = 0.1$): (a) σ_{xx} ; (b) σ_{yy} .

4. Conclusions

The above residual stress analysis with the coupling effect of thermal-plastic deformation and mechanical-plastic deformation yields the following conclusions:

1. The mechanical traction and the ratio of horizontal to vertical forces play an important role in the nature of residual stresses, i.e., tensile or compressive residual stresses.

2. An up-grinding operation is more desirable in terms of the residual stress distribution provided that a low μ and a small input heat flux intensity are maintained.
3. An increase of table speed or that of convection heat transfer coefficient has a similar influence in reducing the residual stresses, if the maximum grinding temperature is kept the same.
4. When the reduction of surface residual stresses is concerned, a down-grinding should be employed.

5. Notations

H	non-dimensional heat-transfer coefficient ($2\alpha h/\kappa v$)
h	heat-transfer coefficient of coolant
L_c	length of grinding zone, see Fig. 1.
l_a	relative peak location of heat flux ($2\zeta_a/L_c$), see Fig. 1
Pe	Peclet number ($vL_c/4\alpha$)
p	vertical traction, see Fig. 1
p_a	peak value of p
q	heat flux per unit grinding width, Fig. 1
q_a	peak value of q
T	temperature rise with respect to ambient temperature
T_∞	
v	moving speed of the heat flux and surface traction, see Fig. 1
κ	thermal conductivity of a workmaterial
Y	yield stress of the workmaterial
α	thermal diffusivity of the workmaterial
ν	Poisson's ratio of the workmaterial
σ	stress tensor
μ	ratio of horizontal to normal traction

Subscripts

e	effective
max	maximum
T	thermal
x, y, z	x -, y -, and z -directions, see Fig. 1
Y	yield
∞	room temperature

Acknowledgements

The financial support to the present study from Australian Research Council is very much appreciated. The ADINA code was used for all of the calculations.

References

- [1] L.C. Zhang, T. Suto, H. Noguchi, T. Waida, An overview of applied mechanics in grinding, *Manufact. Rev.* 5 (1992) 261–273.
- [2] M. Mahdi, L.C. Zhang, The finite element thermal analysis of grinding processes by ADINA, *Comp. Struc.* 56/2–3 (1995) 313–320.
- [3] M. Mahdi, L.C. Zhang, A theoretical investigation on the mechanically induced residual stresses due to surface grinding, progress of cutting and grinding, *JSPE*, vol. III, ICPCG-96, pp. 484–487.
- [4] M. Mahdi, L.C. Zhang, Applied mechanics in grinding—Part V, thermal residual stresses, *Int. J. Mech. Tools Manufact.* 37 (1997) 619–633.
- [5] L.C. Zhang, T. Suto, H. Noguchi, T. Waida, On some fundamental problems in grinding. In: M.A. Aliabadi, C.A. Brebbia (Eds.), *Computer Methods and Experimental Measurements for Surface Treatment Effects*, Computational Mechanics Publications, Southampton, 1993, pp. 275–284.
- [6] L.C. Zhang, T. Suto, H. Noguchi, T. Waida, Applied mechanics in grinding—Part II, Modelling of elastic modulus of wheels, and interface forces, *Int. J. Mach. Tools Manufact.* 33 (1993) 245–255.
- [7] British Iron and Steel Research Association, *The mechanical and physical properties of the British standard on steels*, vol. 2, Pergamon Press, Oxford, UK, 1969.